

Homology modeling and in silico screening of inhibitors for the substrate binding domain of human Siah2: implications for hypoxia-induced cancers

Gopalsamy Anupriya · Kothapalli Roopa · S. Basappa · Yap Seng Chong · Loganath Annamalai

Received: 16 December 2010 / Accepted: 16 February 2011 / Published online: 16 March 2011
© Springer-Verlag 2011

Abstract The three-dimensional (3D) structure of the substrate binding domain (SBD) of human ubiquitin ligase Siah2 (seven in absentia homolog) was constructed based on the homology modeling approach using the Modeller 9v7 program. The molecular dynamics method was utilized to refine the model and it was further assessed by ProSA, three-dimensional structural superposition (3d-SS) and PROCHEK in order to analyze the quality and reliability of the generated model. Furthermore, we predicted the binding pocket of Siah2 and also validated it by both blind and normal docking using a known functional inhibitor, menadione. Using structure-based high-throughput virtual screening, we identified five lead drug-like molecules against the modeled SBD of Siah2 and analyzed its pharmacokinetic properties to identify the potential inhibitors for Siah2. The docking results for menadione and the lead molecules at the ligand binding site of SBD of Siah2 revealed that the residue Ser39 (corresponding to Ser167 in the full-length protein) is consistently involved in strong hydrogen bonding, and

plays an important role in phosphorylation and the enhanced activity of Siah2.

Keywords Homology modeling · Molecular dynamics · Menadione · Virtual screening · Docking · Substrate binding domain · Siah2

Introduction

The growth of solid tumors is associated with poor oxygen supply (hypoxia) within the tumor mass, which triggers a response that is necessary to recruit new vasculature and thus permit tumor cell survival [1, 2]. Ubiquitin ligase Siah2 has been shown to regulate hypoxia response and hence it has been suggested that Siah2 may act as a target for inhibitor development [3]. However, to date, no structural or drug targeting information against SBD of human Siah2 is available. Homology modeling provides a way of constructing the structure of a protein with a “target” from its amino acid sequence and an experimental 3D structure of a related homologous protein (the “template”). Herein, we applied a homology modeling approach to construct the structure of SBD of Siah2.

Siah is a mammalian homolog of seven in absentia (Sina), a drosophila protein which plays a role in eye development [2]. The Siah family of proteins functions as a component of the ubiquitin ligase system, which is involved in polyubiquitination, a process by which the degradation of proteins occurs with the help of three enzymes: E1, E2 and E3. Siah2 comprises the ubiquitin ligase E3 enzymes [4]. Seven in absentia homolog 2 (Siah2) is an important regulator of pathways activated under hypoxic conditions, and is responsible for tumor development [5]. Siah2 contributes to the degradation of

G. Anupriya · K. Roopa · Y. S. Chong · L. Annamalai (✉)
Department of Obstetrics and Gynaecology,
Yong Loo Lin School of Medicine,
National University of Singapore,
10 Lower Kent Ridge Road,
Singapore 119074, Singapore
e-mail: obgannam@nus.edu.sg

L. Annamalai
e-mail: dr.loga108@gmail.com

S. Basappa
Singapore–MIT Alliance for Research and Technology,
Centre for Life Sciences, S16-05-06,
28 Medical Drive,
Singapore 117456, Singapore

multiple targets involved in cell growth, differentiation, angiogenesis, oncogenesis and inflammation [6].

Structurally, Siah2 is a dimeric protein consisting of a RING domain on its N-terminal followed by two novel zinc-finger motifs and a highly conserved substrate-binding domain (SBD) on its C-terminal [6, 7]. The SBD is of importance in the induction of the hypoxia-inducible factor 1 α (Hif-1 α) dependent pathway [8].

Hif-1 α is upregulated when a hypoxic response occurs, which in turn causes the expression of genes including VEGF to recruit new blood vessel growth in that region. However, when this response happens in tumor cells, it promotes vascularization in the tumor cells, leading to the increased growth and metastasis of these cells [2, 5, 8]. Thus, the response of cancer to hypoxia not only sustains tumor growth and survival, but through angiogenesis it also fosters invasion and metastasis [9].

Under normoxic (normal levels of oxygen) conditions, Hif-1 α is subjected to hydroxylation by prolyl hydroxylases 3 (PHD3), which act as a signal for proteasomal degradation. However, under hypoxic conditions, PHD3 proteins are themselves polyubiquitinated and degraded by Siah ubiquitin ligases [10], resulting in increased levels of Hif-1 α [11]. Thus, the ubiquitin ligase Siah2 has been shown to regulate the hypoxia response by regulating the PHD3 involved in the Hif-1 α dependent pathway [8].

Apart from regulating the Hif-1 α pathway, Siah2 was also found to be involved in a Hif-independent pathway by regulating sprouty2 (SPRY2) via the Ras\ERK pathway [12, 13]. Since these pathways are critical in human cancers, it has been suggested that Siah2 may provide a target for the development of inhibitors [3]. In addition, under hypoxic conditions, Siah2 is activity positively regulated by the p38 and Akt pathways through phosphorylation and induction, respectively [14]. Siah2 activity is enhanced by the phosphorylation of serine and threonine residues by the p38 pathway [15, 16]. The mechanism behind the induction of Akt by Siah2 remains unclear [17].

The inhibition of Siah2 expression could effectively inhibit angiogenesis in tumors. In this regard, menadione (vitamin K3) has been identified as an inhibitor for Siah2. This compound effectively attenuates hypoxia and the MAPK signaling pathway and inhibits melanoma growth in the mouse xenograft model [18]. To date no structural or drug targeting information against the SBD of human Siah2 has become available.

In this study, we present structural information on the SBD for Siah2—which may be a novel drug target for studies aimed at developing inhibitors of cancers under hypoxic conditions—using a homology modeling approach followed by a molecular dynamics simulation in order to analyze the stability of this domain. In addition, we predict the binding site of this SBD in order to eventually identify

drug-like molecules that possess enhanced binding energies and pharmacokinetic properties for this SBD using in silico high-throughput virtual screening with menadione as a reference ligand. The potential specific drug-like molecules obtained from such a screening procedure could serve as inhibitors against the SBD of Siah2.

Materials and methods

Homology modeling

Homology modeling of the SBD of Siah2 was performed using Modeller 9v7 software. The amino acid sequence of human Siah2 was retrieved from GenBank (accession number: NM_005067) in NCBI [19]. It consists of 324 amino acids, among which residues 129–322 belong to SBD. The SBD was then subjected to a PSI-BLAST search [20] in order to identify the homologous proteins from the Brookhaven Protein Data Bank (PDB) [21]. An appropriate template for SBD was identified based on the e-value and sequence identity. The template and the target sequences were then aligned using ClustalW [22]. Subsequently, homology modeling was carried out for the SBD of Siah2 against the chosen template using Modeller 9v7 [23]. The outcomes of the modeled structures were ranked on the basis of an internal scoring function, and those with the least internal scores were identified and utilized for model validation.

Validation of the modeled structure

In order to assess the reliability of the modeled structure of Siah2, we calculated the root mean square deviation (RMSD) by superimposing it on the template structure using a three-dimensional structural superposition (3d-SS) tool [24]. The backbone conformation of the modeled structure was calculated by analyzing the phi (Φ) and psi (Ψ) torsion angles using PROCHECK [25], as determined by Ramachandran plot statistics. Finally, the quality of the consistency between the template and the modeled Siah2 was evaluated using ProSA [26], during which the energy criteria for the modeled structure were compared with the potential mean force obtained from a large set of known protein structures.

Protein simulation

The stability of the modeled Siah2 was checked in a molecular dynamics (MD) simulation using the Gromacs software package [27]. The modeled SBD was energy minimized using the Optimized Potentials for Liquid Simulations All-Atom (OPLS) force field [28]. This preliminary energy minimization was done to discard the high-energy intramolecular interactions. The overall geometry and

atomic charges were optimized to avoid steric clashes. The modeled SBD was solvated in a rectangular box of about 16,614 water molecules using the TIP3P model system in order to mimic the physiological behavior of the molecules [29].

The energy of the modeled Siah2 was then minimized without restraints for 2000 steps using the abovementioned algorithms. The system was then gradually heated from 10 to 300 K over 5 ns using the NVT ensemble. Finally, an MD simulation was carried out to examine the quality of the modeled structures by checking their stability and performing a 5 ns simulation, and the lowest-energy structure found during the simulation was calculated. A similar protocol was followed for the template in order to compare the stabilities and reliabilities of the modeled and experimentally solved proteins.

Docking studies

SBD of Siah2 was modeled computationally and its active sites were predicted using SiteMap (version 2.3, 2009, Schrödinger, LLC, New York, USA) followed by docking studies. The preparation of the modeled Siah2 was achieved by a protein preparation wizard, menadione was prepared using the LigPrep program, and the docking procedure was performed using Extra Precision (XP) Glide (version 5.5, 2009, Schrödinger, LLC), which produces the least number of inaccurate poses and calculates the accurate binding energy of the 3D structure of a known protein with a ligand [30–32]. Docking studies were carried out using menadione as an inhibitor against the modeled SBD of Siah2. Since menadione seemed to be a promising functional inhibitors against Siah2, we initially docked with the putative binding site of Siah2. The Siah2–menadione ligand complex was used as a reference point in order to identify the drug-like molecules that could usefully interact with the SBD of Siah2. The *in silico* structure-based high-throughput virtual screening (HTVS) method was used to identify potential small-molecule inhibitors using 14,400 drug-like subsets obtained from the Maybridge database (<http://www.maybridge.com>) against the putative active site of SBD of Siah2. The lead molecules from screening were then tested *in silico* for their pharmacokinetic properties and their percent human oral absorption values using QikProp (version 3.2, 2009, Schrödinger, LLC) [33].

Results and discussion

Homology modeling of Siah2 and its evaluation

The main criteria in homology modeling are template selection and sequence alignment between the target and

the template. The PDB IDs for the three template hits that were found for the SBD of Siah2 after performing PSI-Blast were 1K2F, 2AN6 and 2A25. The 3D structure of 2AN6 has a very high resolution and there are 13 missing residues in its X-ray structure. Although 2A25 seems to be a good template with low resolution, its 15 missing residues appear as a string in the modeled protein. Therefore, 1K2F was identified as a promising template that had a sequence similarity of 86% to the SBD with a resolution of 2.4 Å and contained no missing residues. Hence, the structure 1K2F was selected as the appropriate template for SBD modeling. During modeling, the original amino acid positions of the SBD (i.e., 129–322) were re-labeled as residues 1–193, respectively, by Modeller 9v7. These latter residues were considered in further data analysis.

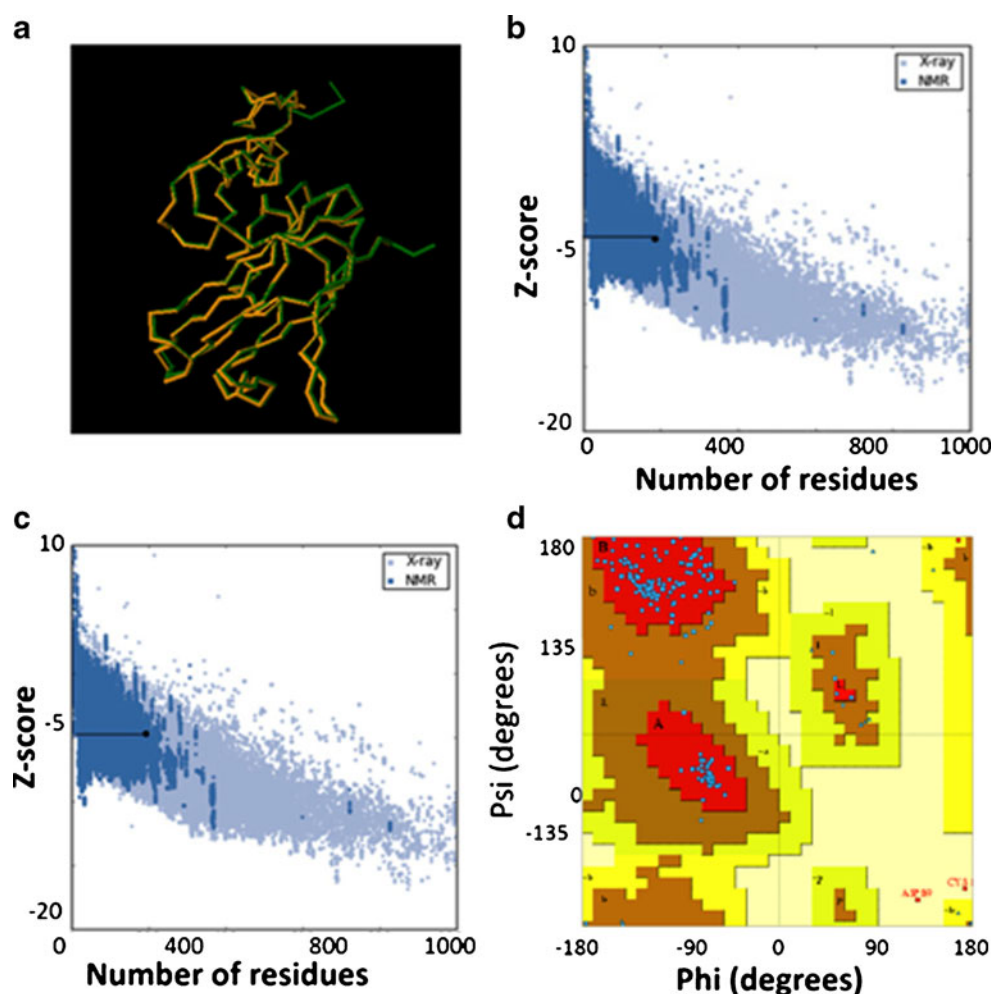
Twenty-five models were generated and ranked during the modeling of SBD against the template 1K2F. The best-ranked model (Fig. 1) was then subjected to evaluation to check the quality of the generated model.

The modeled SBD of Siah2 was used for further optimization and validation. The calculated root mean square deviation between the target and template structure was found to be 0.324 Å (Fig. 2a). Furthermore, the quality of the structure derived from homology modeling was validated by calculating the ProSA Z-score, which gives the overall model quality based on the C α positions. The Z-scores of the target and template were –4.7 and –5.2. Hence, the



Fig. 1 Modeled structure of the SBD of Siah2 obtained from Modeller 9v7. The structure is shown in secondary structure mode using Pymol; the α -helices, β -sheets and loops are colored *red*, *yellow* and *green*, respectively

Fig. 2 **a** Superimposition of modeled Siah2 (target) on 1K2F (template) using the 3d-SS tool. In this wireframe diagram, *yellow* represents the target and *green* represents the template. **b** This plot that contains the Z-scores of all experimentally determined protein chains in the current PDB that have been solved by either X-ray diffraction or NMR. The Z-score of -4.7 indicated on this graph represents the overall quality of the modeled 3D structure of Siah2. This plot can be used to check whether the Z-score of this 3D structure is within the range of scores typically found for native proteins of a similar size. **c** The Z-score of -5.1 indicated on this graph represents the overall quality of the template's 3D structure (PDB ID 1K2F). When compared to Fig. 2b, it was found that the overall quality of the 3D structure of the template and that of the target are very similar in terms of their Z-scores. **d** Ramachandran plot for the modeled SBD of Siah2. The most favored regions are colored *red*; additional allowed, generously allowed and disallowed regions are shown as *yellow*, *light yellow* and *white* fields, respectively



quality of the model obtained was validated using the ProSA score. Both the target and the template models show similar profiles, as seen in Fig. 2b, c.

Geometric evaluations of the modeled 3D structure of SBD were performed using PROCHECK by calculating the Ramachandran plot (Fig. 2d) (Table 1). This plot represents the distribution of the phi and psi angles for the amino acid residues. The percentage of phi and psi angles that occur in

the allowed regions was 90% for residues in the core region, whereas this percentage was 0.9% for the residues located in the disallowed regions.

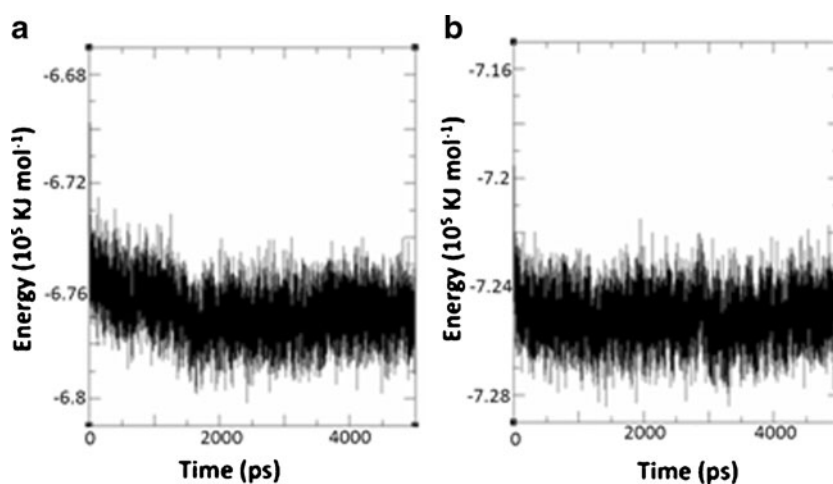
Simulation and docking

The stability of the modeled SBD of Siah2 was assessed by MD simulation for 5 ns, and was used for subsequent docking studies. In addition, parameters such as pressure, temperature and total energy were calculated to check the stability of the modeled protein with improved steric parameters. The analysis of the simulation parameters revealed that the total energy for the modeled SBD is -6.74×10^5 kJ mol⁻¹ and that for the template 1K2F is -7.22×10^5 kJ mol⁻¹ (Fig. 3a, b). This shows that the target and template have similar total energies, so the modeled structure was considered to be as stable as the experimentally solved structure of the template (1K2F). Applying a pressure of 1.0 bar and a temperature of 300K to both proteins did not result in any significant difference until 5 ns. Based on these simulation parameters, it is evident that the modeled SBD has good conformational stability, and could serve as a potential drug target.

Table 1 Ramachandran plot statistics for the 3D model of SBD of Siah2, calculated using PROCHECK

Parameter	Value
Core (%)	90.3
Allowed (%)	0.8
General (%)	0.6
Disallowed (%)	0.9
Bad contacts	12
G factor	-0.02
Main chain bond lengths	-0.17
Main chain bond angles	-0.23

Fig. 3 The total energies of the modeled SBD of Siah2 (a) and the template 1K2F (b) were compared using Gromacs. This comparison shows that the overall energies of the target and template are very similar, so the modeled SBD was considered to be as stable as the experimentally solved structure of the template (1K2F)



The validated and refined model was then used for docking with a known functional inhibitor, menadione, and the complexes were analyzed for the putative functional amino acid residues that are involved in hydrogen bonding. Prediction of the binding site of SBD was performed using Sitemap in Schrodinger, which yields 13 amino acid residues in the binding pocket of SBD for Siah2 (Fig. 4). The predicted binding pocket was validated using Glide (XP) by performing both blind docking (to examine whether the ligand binds to the protein away from the predicted binding site) and normal docking (allowing the ligand to bind to the predicted binding site) with menadione used as the inhibitor of Siah2. It was observed that 8 of the 13 predicted binding site atoms were within 5 Å of the ligand in both docking procedures.

In addition, we observed that the amino acid Ser39 (corresponding to Ser167 in the full-length protein) is involved in hydrogen-bond formation with menadione during both of the docking procedures. This particular binding site was utilized for HTVS of compounds from a Maybridge database. As a result, 1000 potential ligand hits were identified based on their pharmacokinetic properties (ADMET). Subsequently, 156 drug-like molecules were

identified that had better Glide scores than menadione, and these were compared with its binding conformation; eventually 20 lead molecules were selected. Five of these 20 drug-like molecules were identified as potential lead molecules for inhibition of Siah2 based on their hydrogen-bonding interactions with the putative functional amino acid residue Ser39 (with binding energies ranging from around -6 kcal mol $^{-1}$ to around -8 kcal mol $^{-1}$; the binding energy for menadione is approximately -5 kcal mol $^{-1}$). The chemical structures of these lead molecules are presented along with their IUPAC names in Fig. 5.

The conformations of these lead compounds when binding to the modeled Siah2 were also analyzed to determine the hydrogen-bond interactions (Fig. 6). All protein–ligand complexes for these five lead molecules possess multiple hydrogen bonds when compared with menadione. It is worth noting that all five lead molecules interact with residue Ser39, and their respective Glide scores are comparable to that of menadione. The docking results for the final lead molecules against Siah2 are given in Table 2.

The drug-like properties of the lead compounds was assessed by evaluating their physicochemical properties using

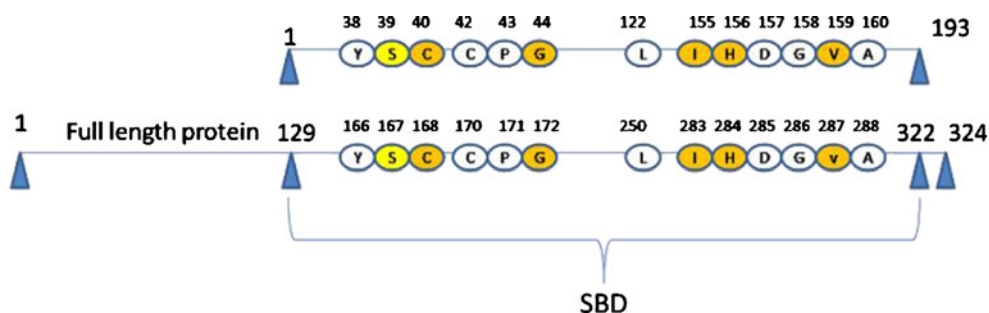


Fig. 4 The 13 predicted active site residues of SBD. The amino acids in the SBD were numbered from 1 to 193 during modeling, whereas the corresponding amino acid residue positions for the full-length protein are also shown (amino acid residues 1–324). The *yellow* color

represents amino acid that is consistently involved in hydrogen-bond formation for all five identified lead molecules, whereas the *orange* color represents the other amino acids involved in hydrogen bonding

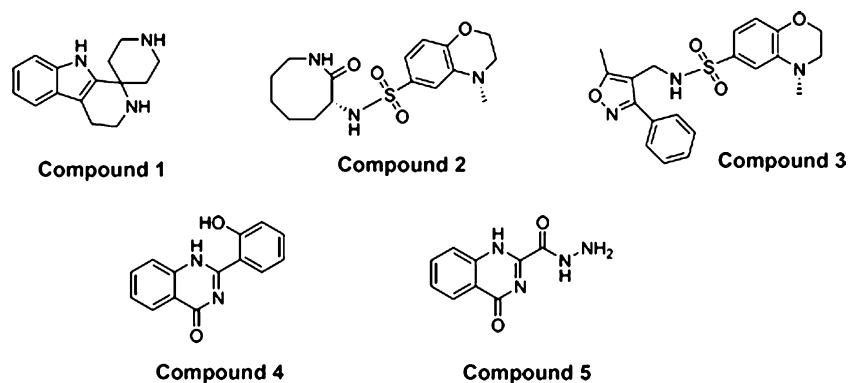


Fig. 5 Structures of the five lead molecules along with their corresponding Maybridge IDs. Compound 1 (7599): 2',3',4',9'-tetrahydrospiro[piperidine-4,1'-pyrido[3,4-b]indole]; compound 2 (724): (*R*)-4-methyl-*N*-(2-oxoazocan-3-yl)-3,4-dihydro-2*H*-benzo[b][1,4]oxazine-6-sulfonamide; compound 3 (4035): 4-methyl-*N*-

((5-methyl-3-phenylisoxazol-4-yl)methyl)-3,4-dihydro-2*H*-benzo[b][1,4]oxazine-6-sulfonamide; compound 4 (10746): 2-(2-hydroxyphenyl) quinazoline-4(1*H*)-one; compound 5(7757): 4-oxo-1,4-dihydroquinazoline-2-carbohydrazide

QikProp [34]. Their molecular weights were <500 Da; they had <5 hydrogen bond donors and <10 hydrogen bond acceptors, and $\log P$ values of <5 (Table 3). These properties are all well within the acceptable range of Lipinski's rule of

five. Further, the pharmacokinetic parameters of the lead molecules were analyzed, including their absorption, distribution, metabolism, excretion and toxicity (ADMET), using QikProp. For the five lead compounds, the partition

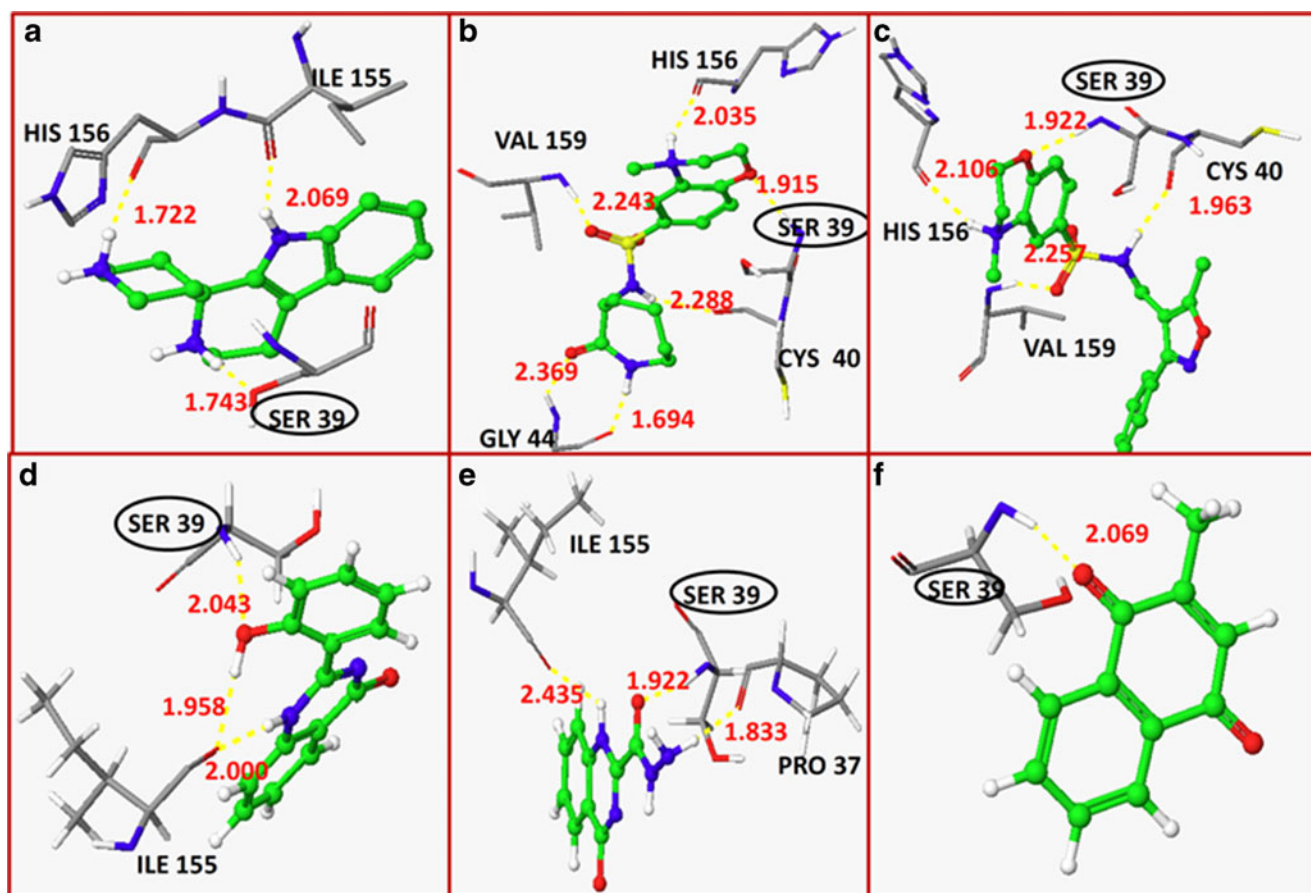


Fig. 6 Binding poses of the five lead molecules. The proposed binding modes of the lead molecules are shown in ball and stick format, and non-carbon atoms are colored by atom type. Critical residues for binding are shown as tubes colored by atom type. Hydrogen bonds are shown as

dotted yellow lines, and the distance between the donor and acceptor atoms is indicated. Atom type color code: red for oxygen, blue for nitrogen, gray for carbon, and yellow for sulfur atoms. The Ser39 amino acid residue that interacts with each lead molecule is indicated by a circle

Table 2 Extra Precision (XP) Glide results for the five lead molecules and menadione, obtained using Schrodinger 9.0

Lead molecules ^a	Glide score (kcal/mol) ^b	Amino acids involved in interactions	No. of HBs ^c
7599	-8.3618	SER39, ILE155 and HIS156	3
724	-7.4965	GLY44, VAL159, CYS40, SER39 and HIS156	6
4035	-6.7967	SER39, CYS40, HIS156 and VAL159,	4
10746	-6.5975	SER39 and ILE155	3
7757	-6.5049	SER39, ILE155 and PRO37	3
Menadione	-5.6476	SER39	1

^a Ligand IDs are from the Maybridge database

^b Glide score

^c Number of hydrogen bonds formed

coefficient ($QPlogP_{o/w}$) and water solubility ($QPlogS$) values, which are crucial for estimating the absorption and distribution of drugs within the body, ranged from approximately -0.9 to 2.23 and -0.05 to -3.65, respectively, while the bioavailability and toxicity values were around -0.1 to 0.3. Overall, the percent human oral absorption values for the compounds ranged from approximately 57 to 72%. These pharmacokinetic parameters are well within the acceptable range defined for human use, thereby indicating their potential as drug-like molecules.

The identified Siah2 inhibitors may block the interaction between Siah2 and PHD3 (protein–protein interaction), or they could bind to functionally important residues like serine and threonine that are involved in phosphorylation, thereby enhancing Siah2 activity [15, 16]. Hence, we hypothesize that these lead drug-like small molecules could serve as inhibitors against Siah2. Given that this study

mainly aimed to find compounds that could block the protein–protein interaction with no catalytic activity, it is worth noting that these small molecules possessed greater binding affinity than menadione to Siah2. However, more studies are needed to reinforce these findings.

Conclusions

Our study provided the 3D structure of Siah2 through a homology modeling approach. Energy minimization and molecular dynamics simulations were done to check the stability of the modeled structure. Analysis of the results of the homology modeling and MD simulations indicated that the theoretical predictions were consistent with the known set of experimental results. Using HTVS, we identified five drug-like molecules with better binding affinities than

Table 3 QikProp properties of the identified drug-like molecules and menadione, obtained using Schrödinger 9

Lead molecules ^a	$QPlogP_{o/w}$ ^b	$QPlogS$ ^c	MW ^d	$QPlogHERG$ ^e	No. of metab. ^f	HA ^g	HD ^h	Percent human oral absorption ⁱ
7599	1.771	-1.251	241.33	-5.708	1	5	3	72.335
724	0.845	-2.075	339.41	-6.651	3	7	2	74.975
4035	3.008	-4.930	339.46	-5.765	4	7	1	77.055
10746	1.842	-3.058	238.24	-5.360	2	4	2	70.148
7757	-0.523	-1.966	204.188	-5.416	0	6	3	55.280
Menadione	-0.967	-1.051	198.671	-6.351	4	6	4	57.45

^a Ligand IDs are from the Maybridge database

^b Predicted octanol/water partition coefficient $\log P$ (acceptable range: -2.0 to 6.5)

^c Predicted aqueous solubility S in mol/L (acceptable range: -6.5 to 0.5)

^d Molecular weight (<500 Da)

^e Predicted IC_{50} value for blockage of HERG K⁺ channels (acceptable range: below -5.0)

^f Number of metabolic reactions (1–8)

^g Hydrogen bond acceptors (<10)

^h Hydrogen bond donors (<5)

ⁱ Percent human oral absorption (<25% is poor and >80% is high)

menadione to Siah2. Further analysis of the binding conformations of the lead molecules revealed that the Ser39 residue of the SBD may be the key amino acid residue that interacts with the ligands needed to induce Siah2 activity. However, further experimental studies are required to prove the therapeutic potentials of these lead drug-like small molecules.

Acknowledgments We gratefully acknowledge a generous grant from the Lee Foundation, Singapore, for this study.

References

- Nakayama K (2009) Cellular signal transduction of the hypoxia response. *J Biochem* 146:757–765
- Nakayama K, Qi J, Ronai Z (2009) The ubiquitin ligase Siah2 and the hypoxia response. *Mol Cancer Res* 7:443–451
- House CM, Moller A, Bowtell DD (2009) Siah proteins: novel drug targets in the Ras and hypoxia pathways. *Cancer Res* 69:8835–8838
- Schnell JD, Hicke L (2003) Non-traditional functions of ubiquitin and ubiquitin-binding proteins. *J Biol Chem* 278:35857–35860
- Nakayama K, Frew IJ, Hagensen M, Skals M, Habelhah H, Bhoumik A, Kadoya T, Erdjument-Bromage H, Tempst P, Frappell PB, Bowtell DD, Ronai Z (2004) Siah2 regulates stability of prolyl-hydroxylases, controls HIF1alpha abundance, and modulates physiological responses to hypoxia. *Cell* 117:941–952
- House CM, Hancock NC, Moller A, Cromer BA, Fedorov V, Bowtell DD, Parker MW, Polekhina G (2006) Elucidation of the substrate binding site of Siah ubiquitin ligase. *Structure* 14:695–701
- Polekhina G, House CM, Traficante N, Mackay JP, Relaix F, Sassoon DA, Parker MW, Bowtell DD (2002) Siah ubiquitin ligase is structurally related to TRAF and modulates TNF-alpha signaling. *Nat Struct Biol* 9:68–75
- Qi J, Nakayama K, Gaitonde S, Goydos JS, Krajewski S, Eroshkin A, Bar-Sagi D, Bowtell D, Ronai Z (2008) The ubiquitin ligase Siah2 regulates tumorigenesis and metastasis by HIF-dependent and -independent pathways. *Proc Natl Acad Sci USA* 105:16713–16718
- Brizel DM, Scully SP, Harrelson JM, Layfield LJ, Bean JM, Prosnitz LR, Dewhirst MW (1996) Tumor oxygenation predicts for the likelihood of distant metastases in human soft tissue sarcoma. *Cancer Res* 56:941–943
- Moller A, House CM, Wong CS, Scanlon DB, Liu MC, Ronai Z, Bowtell DD (2009) Inhibition of Siah ubiquitin ligase function. *Oncogene* 28:289–296
- Huang J, Tsvetkov L, Qu K, Daniel-Issakani S, Payan DG (2008) Approaches to discovering drugs that regulate E3 ubiquitin ligases. *Ernst Schering Found Symp Proc* 153–170
- Nadeau RJ, Toher JL, Yang X, Kovalenko D, Friesel R (2007) Regulation of Sprouty2 stability by mammalian Seven-in-Absentia homolog 2. *J Cell Biochem* 100:151–160
- Shaw AT, Meissner A, Dowdle JA, Crowley D, Magendanz M, Ouyang C, Parisi T, Rajagopal J, Blank LJ, Bronson RT, Stone JR, Tuveson DA, Jaenisch R, Jacks T (2007) Sprouty-2 regulates oncogenic K-ras in lung development and tumorigenesis. *Genes Dev* 21:694–707
- Seta KA, Spicer Z, Yuan Y, Lu G, Millhorn DE (2002) Responding to hypoxia: lessons from a model cell line. *Sci STKE* 146:re11
- Khurana A, Nakayama K, Williams S, Davis RJ, Mustelin T, Ronai Z (2006) Regulation of the ring finger E3 ligase Siah2 by p38 MAPK. *J Biol Chem* 281:35316–35326
- Emerling BM, Platanius LC, Black E, Nebreda AR, Davis RJ, Chandel NS (2005) Mitochondrial reactive oxygen species activation of p38 mitogen-activated protein kinase is required for hypoxia signaling. *Mol Cell Biol* 25:4853–4862
- Zundel W, Schindler C, Haas-Kogan D, Koong A, Kaper F, Chen E, Gottschalk AR, Ryan HE, Johnson RS, Jefferson AB, Stokoe D, Giaccia AJ (2000) Loss of PTEN facilitates HIF-1-mediated gene expression. *Genes Dev* 14:391–396
- Shah M, Stebbins JL, Dewing A, Qi J, Pellicchia M, Ronai ZA (2009) Inhibition of Siah2 ubiquitin ligase by vitamin K3 (menadione) attenuates hypoxia and MAPK signaling and blocks melanoma tumorigenesis. *Pigment Cell Melanoma Res* 22:799–808
- McGinnis S, Madden TL (2004) BLAST: at the core of a powerful and diverse set of sequence analysis tools. *Nucleic Acids Res* 32:W20–25
- Altschul SF, Madden TL, Schaffer AA, Zhang J, Zhang Z, Miller W, Lipman DJ (1997) Gapped BLAST and PSI-BLAST: a new generation of protein database search programs. *Nucleic Acids Res* 25:3389–3402
- Berman H, Henrick K, Nakamura H (2003) Announcing the worldwide Protein Data Bank. *Nat Struct Biol* 10:980
- Thompson JD, Gibson TJ, Higgins DG (2002) Multiple sequence alignment using ClustalW and ClustalX. *Curr Protoc Bioinformatics* Aug:2.3
- Sali A, Blundell TL (1993) Comparative protein modelling by satisfaction of spatial restraints. *J Mol Biol* 234:779–815
- Sumathi K, Ananthalakshmi P, Roshan MN, Sekar K (2006) 3dSS: 3D structural superposition. *Nucleic Acids Res* 34:W128–132
- Laskowski RA, MacArthur MW, Moss DS, Thornton JM (1993) PROCHECK: a program to check the stereochemical quality of protein structures. *J Appl Cryst* 26:283–291
- Wiederstein M, Sippl MJ (2007) ProSA-web: interactive web service for the recognition of errors in three-dimensional structures of proteins. *Nucleic Acids Res* 35:W407–410
- Hess B, Kutzner C, van der Spoel D, Lindahl E (2008) GROMACS 4: algorithms for highly efficient, load-balanced, and scalable molecular simulation. *J Chem Theor Comput* 4:435–447
- McDonald NA, Jorgensen WL (1998) Development of an all-atom force field for heterocycles. Properties of liquid pyrrole, furan, diazoles, and oxazoles. *J Phys Chem B* 102:8049–8059
- Jorgensen W, Chandrasekhar J, Madura J, Impey R, Klein M (1983) Comparison of simple potential functions for simulating liquid water. *J Chem Phys* 79:926–935
- Kontoyianni M, McClellan LM, Sokol GS (2003) Evaluation of docking performance: comparative data on docking algorithms. *J Med Chem* 47:558–565
- Schrodinger, LLC (2005) Glide: molecular docking tool, v.4.0. Schrodinger, LLC, New York
- Friesner RA, Banks JL, Murphy RB, Halgren TA, Klicic JJ, Mainz DT, Repasky MP, Knoll EH, Shelley M, Perry JK, Shaw DE, Francis P, Shenkin PS (2004) Glide: a new approach for rapid, accurate docking and scoring. 1. Method and assessment of docking accuracy. *J Med Chem* 47:1739–1749
- Jorgensen WL (2006) QikProp, v.3.0. Schrodinger, LLC, New York
- Lipinski CA, Lombardo F, Dominy BW, Feeney PJ (2001) Experimental and computational approaches to estimate solubility and permeability in drug discovery and development settings. *Adv Drug Deliv Rev* 46:3–26